Article

Validation of Sentinel-3 SAR Level-2 and Level-3 Products in the Baltic Sea and Estonian lakes

Aive Liibusk[1,*], Tarmo Kall[1], Sander Rikka[2], Rivo Uiboupin[2], Ülo Suursaar[3], Kuo-Hsin Tseng[4,5]

[1] Estonian University of Life Sciences, Chair of Geomatics, Tartu 51006, Estonia
[2] Department of Marine Systems at Tallinn University of Technology, Tallinn 12618, Estonia
[3] Estonian Marine Institute, University of Tartu, Tallinn 12618, Estonia
[4] Center for Space and Remote Sensing Research, National Central University, Taoyuan 32001, Taiwan
[5] Institute of Hydrological and Oceanic Sciences, National Central University, Taoyuan 32001, Taiwan
* Correspondence: aive.liibusk@emu.ee; Tel.: +372-7313-196 (A.L.)

Abstract: Multimission satellite altimetry (e.g. ERS, Envisat, TOPEX/Poseidon, Jason) data have enabled a synoptic view of ocean variations in the past decades, including sea-level rise and mesoscale circulations. Since 2016, the Sentinel-3 mission has provided better spatial and temporal sampling compared with its predecessors. The Sentinel-3 Ku/C Radar Altimeter (SRAL) is one of the synthetic aperture radar altimeters (SAR Altimeter) which is more precise in coastal and lake observations. In this study, we validate Sentinel-3 Level-2 products in Baltic Sea coastal areas and two lakes in Estonia. Moreover, the Copernicus Marine Environment Monitoring Service (CMEMS) Level-3 sea-level anomaly data and the Nucleus for European Modelling of the Ocean (NEMO) reanalysis model outcomes are compared with measurements from a tide gauge network. A dense *in situ* water level network deployed along the coast for geodetic observation was utilised to provide ground truths for validating altimetry results. Three validation methods were used for Level-2 data: *(i)* collocated Sentinel-3 and GNSS ship measurements; *(ii)* a national geoid model (EST-GEOID2017) with sea-level anomaly correction; *(iii)* collocated Sentinel-3 and buoy measurements. The validations were carried out in seven Sentinel-3A/B overpasses in 2019. Our results show that the uncertainty of the Sentinel-3 Level-2 altimetry product is below decimetre level on the Estonian coast and the targeted lakes. Results from CMEMS Level-3 showed a correlation of 0.8 (RMSE 0.19 m) and 0.91 (RMSE 0.27 m) when compared against tide gauge measurements and NEMO model, respectively.

Keywords: Sea level; GNSS; NEMO reanalysis; tide gauges; pressure buoys; geoid model; CMEMS; Copernicus

1. Introduction

Tide gauges (TG) have been widely deployed to register sea-level variations on the coast, and their time series are considered longer and more reliable than other remote sensing measurements. However, the records might be contaminated by several effects, such as glacial isostatic adjustment (GIA), neotectonic movements and local land subsidence. Tide gauge networks are usually sparsely distributed along the shoreline and their measurements are related to the land with surface deformation they are connected to. To avoid the above-mentioned influences and to transform sea surface heights (SSHs) into a common height system, it is recommended to use GNSS tide gauges or satellite altimetry to calculate the absolute SSH above a reference ellipsoid [1, 2]. A radar altimeter is a precise ranging tool designed for measuring SSH over the open ocean at an uncertainty level of around 3.5-5 cm [1, 3, 4]. Satellite altimetry has been used in sea-level variation studies for more than 30 years; it was evolved from the experimental Seasat mission in the late 1970s and gained popularity in the 1990s when TOPEX/Poseidon and ERS-1 missions were launched. Nowadays, it is a very important tool for understanding the topography of mesoscale eddies and the multidecadal trend of eustatic (global) sea-level rise.

Today, altimetry is not only an irreplaceable tool for the open ocean but also for gaining visibility in order to monitor regional and coastal mean sea-level (MSL) trends, where satellite data complement *in situ* TG time series and hydrodynamic models. Major progress was made over the last 15 years thanks to several innovative retracking algorithms in the coastal zone. Success has been furthered by the development of the Synthetic Aperture Radar Altimeter (SAR Altimeter), which performs coherent processing of groups of transmitted pulses and exploits the Delay Doppler signal of the full bandwidth [5]. The progress of altimetry data processing methods has also been driven by the improvement of geophysical corrections, such as wet/dry troposphere corrections, ionospheric delay, tidal models as well as the necessary waveform retracking algorithms [6]. Additionally, several new-generation radar altimeters were launched in the last decades. For example, CryoSat-2 was launched in 2010 [7] and the two satellites of the Sentinel-3A/B (S3A/B) constellation were launched in 2016 and 2018, respectively. This new altimetry fleet provides much higher spatial resolution and lower noise, aiming at reducing land contamination in coastal radar echoes. CryoSat-2 and Sentinel-3 operating in SAR mode have a waveform footprint of 5 km², much smaller than that covered by pulse-limited altimeters in 20-30 km², such as SARAL/AltiKa and the Jason series. The along-track resolution of SAR altimeters has been increased to approximately 300 m along the flight path [8].

However, the accuracy of coastal altimetry is still affected by the ratio between the targeted water and the neighbouring terrain within a footprint [9]. It has been demonstrated that SSH could be estimated to decimetre-level accuracy in the Baltic Sea [10] and to a couple of decimetres for small lakes with diameter less than 10 km using SAR altimeters [11]. Various validation methods are able to determine the accuracy of altimetric heights. For instance, Etcheverry et al. [12] used 478 global tide gauges to verify gridded altimetry sea-level anomaly (SLA) [12], while Ardalan et al. [13] deployed GPS buoys to evaluate SARAL/AltiKa produces, Birgiel et al. [10] used the precise national geoid model to examine Sentinel-3 coastal product with a SAMOSA 2 retracker and Bonnefond et al. [14] used a GPS-catamaran. All of these methods can be cross-validated as well.

The main objective of this study was to validate Sentinel-3A and Sentinel-3B Level-2 altimetry products along the Estonian coast of the Baltic Sea and in two small lakes: Võrtsjärv and Lake Peipus. The second(ary) aim was to evaluate the accuracy of Level-3 altimetry products as well as the Nucleus for European Modelling of the Ocean (NEMO) reanalysis model results, which are available through the Copernicus Marine Environment Monitoring Service (CMEMS) service.

2. Material and Methods

2.1. Validation Scheme

In this study, five validation strategies, including two field campaigns conducted in 2019, were investigated. Sea surface height above the ellipsoid GRS80 was determined using: *(i)* GNSS kinematic measurements on the vessel; *(ii)* an offshore buoy equipped with a pressure sensor; *(iii)* the national precise geoid model EST-GEOID2017 corrected with SLA from the four nearest tide gauges. Additionally, correlation analyses between satellite-based and tide gauge-based SLA were carried out using Level-3 data.

An overview of our validation strategy is outlined in Figure 1. In general, Sentinel-3 Level 2 observations were validated with GNSS vessel campaigns, buoy data and the geoid model in designated locations with a relatively short time period in 2019. CMEMS Level 3 data and the NEMO reanalysis model are compared with tide gauges in the Gulf of Finland and the Gulf of Riga in multiple years. More details will be introduced later.
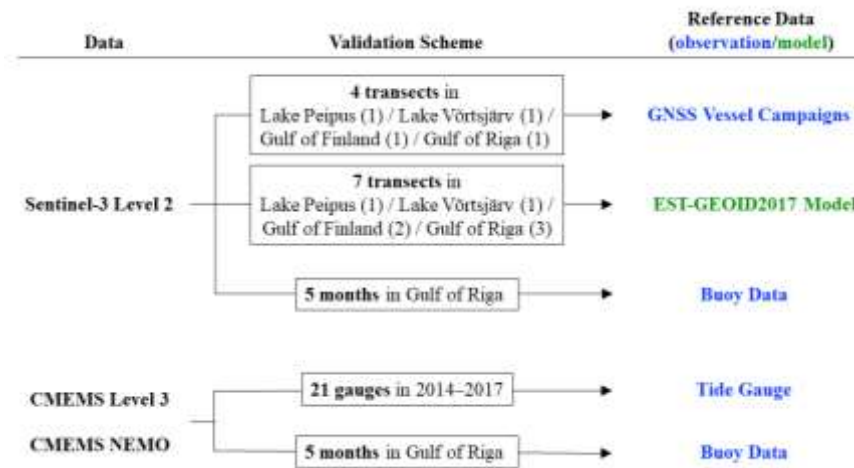
Figure 1. Design of validation and comparison scenarios.

2.2. Study sites

The Baltic Sea is a semi-enclosed water body dotted with thousands of islands and islets. Our study area is in the eastern part of the Baltic Sea (Figure 2), including the Gulf of Finland and the Gulf of Riga. The topography of the southern coast of the Gulf of Finland is varying. There is a 55-metre-high cliff in the east of Kunda (cf. tide gauge number 2 in Figure 2) and a flat seashore along the entire western coast. Steep terrain near the coast can cause peaky waveforms and hinder the performance of retracking algorithms. The Gulf of Riga has a very shallow and sandy seashore. There are many islands in the northern part of the Gulf which also make the altimetry measurements challenging along the fragmental pass-overs.

Lake Peipus (Lake Peipsi) and Lake Võrtsjärv are the two largest lakes in Estonia (Figure 2), with a surface area of 3555 km² and 270 km², respectively. Lake Peipus is the fifth largest lake in Europe, with an average depth of 7.1 m and a max depth of 15.3 m. Võrtsjärv is very shallow with an average depth of 2.7 m and a maximum depth of only 6 m.

Four GNSS transects were selected for Sentinel-3 validation, as shown in Figure 2. The following criteria were taken into consideration in order to choose the transects to conduct GNSS vessel measurements: *(i)* at least one transect has to run over the selected waterbodies (Gulf of Finland, Gulf of Riga, Lake Peipus and Võrtsjärv); *(ii)* both Sentinel-3A (S3A) and Sentinel-3B (S3B) transects would be used; *(iii)* the GNSS measurements on the boat and the buoy measurements could be carried out at the transect. S3B pass 321 crosses over Lake Peipus (leaving the 35 km GNSS transect to the west). One S3B track (pass 528) runs over Lake Võrtsjärv and the pass is close (<3 km) to the reedy coast.

In addition, S3A pass 186 (Gulf of Riga) and S3B pass 625 (Gulf of Finland) in the Baltic Sea were selected for our GNSS vessel campaigns. Three additional transects were added to the selection in order to increase the reliability of the validation results: S3A pass 397 and S3B pass 397 in the Gulf of Riga and S3A pass 186 in the Gulf of Finland (Figure 2). This selection was based on the following criteria: *(i)* the same transect (S3A pass 186) has to run over two water bodies (Gulf of Riga, Gulf of Finland); *(ii)* both S3A and S3B have to pass over the same waterbody (S3A_186 and S3B_397 over the Gulf of Riga); *(iii)* the crossing point of ascending and descending tracks should emerge. This choice helps verify the validation results over various areas and missions in the same water body.
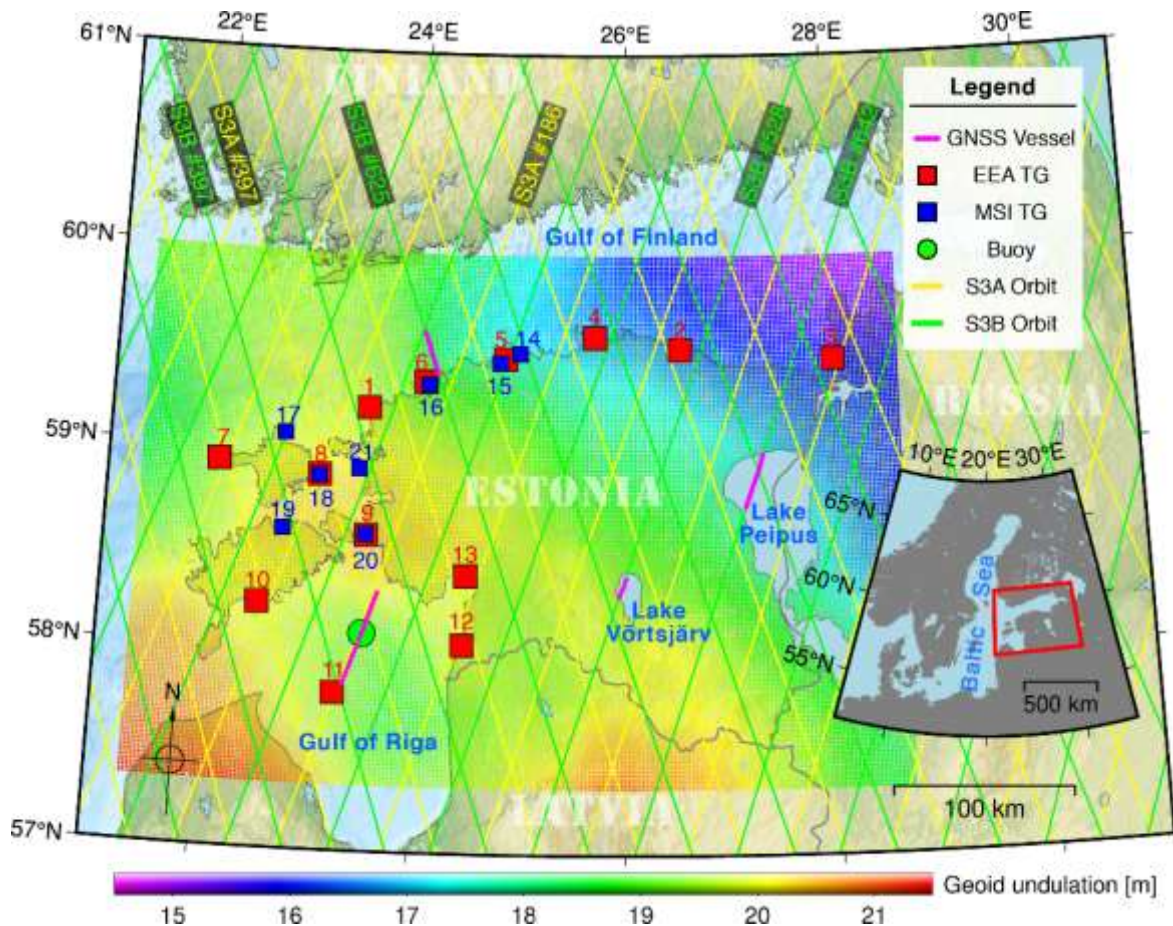
Figure 2. Study area with Sentinel-3 overpasses, tide gauges (red and blue squares), a buoy (green circle) and four GNSS tracks (magenta lines). The labelled Sentinel-3 overpasses were used for validation. The tide gauges are operated by the Estonian Environmental Agency (EEA TG) and the Department of Marine Systems of Tallinn University of Technology (MSI TG). Estonian geoid model EST-GEOID2017 is laid over Estonia.

2.3. Geoid model EST-GEOID2017

Since sea-level variations of tidal origin are less than 10 cm in the study area of the Baltic Sea [15], the precise geoid model is one of the best reference surfaces for validating altimetric heights. The Estonian geoid model (EST-GEOID2017) is a quasi-geoid model covering 57°N-60°N and 20°E-30°E, with a spatial resolution of 1' x 2'. Its long-wavelength information refers to the GOCO05s global gravity model [16]. Additionally, nearly 50,000 gravity points were used with an average formal uncertainty of 0.75 mGal, whereas within Estonian mainland and islands, the uncertainty of gravity data is mostly within 0.5 mGal (see [17] for more details). The EST-GEOID2017 model is very smooth in the mainland (Figure 2) and its GNSS-levelling-based accuracy remains within ±0.005 m [17]. This means that the accuracy of the geoid model in the coastal zones of the lakes should also be around ±0.005 m. Note that the estimated discrepancy of ±0.028 m between the model and the GNSS measurements is estimated in the Gulf of Finland [18]. Having such superb accuracy, the use of the model for satellite altimetry validation in the coastal zones is justified.

Since the validation result depends not only on the accuracy of the altimetry data but also on other factors, the accuracy of the geoid, tide gauge data and GNSS-data should also be taken into consideration. Note that the pressure sensor-based tide gauges are affected by time-dependent drift and need to consider employing control readings from the staff gauge. Therefore, the uncertainty of automatic tide gauges remains in 1-2 cm level [19]. The accuracy of the GNSS height component depends on several factors, such as the antenna and receiver, the method of measurement and

processing. However, the GNSS height component accuracy on the vessel, based on the kinematic method, remains within a ±2 cm level as well [18].

2.4. Sentinel-3 data products

Sentinel-3 satellites carry a dual-frequency SAR altimetry payload. The main frequency used for range measurements is Ku-band (13.575 GHz), while the C-band (5.41 GHz) is used for ionospheric correction. The SRAL altimeter has high resolution in the along-track (300 m) and across-track (1.64 km) directions, which gives better results in the coastal areas [20] compared with the conventional pulse-limited radar altimeter. Sentinel-3 is operating in a sun-synchronous orbit with a repeat cycle of 27 days. Combining S3A and S3B, the repeat cycle between two satellites on a regional scale becomes 13.5 days and the interval between interleaved groundtracks is 27 km near the Equator, which offers a better temporal and spatial resolution and also increases the chance of passing over small waterbodies.

For this study, Sentinel-3 SRAL Non Time Critical Level-2 data (SR_2_LAN) from the Estonian National Copernicus Hub (ESTHub) mirror site (https://ehdatahub.maaamet.ee/dhus/#/home) in the period from Dec 2018 to Nov 2019 were used. Note that the radar range (R) measured between the satellite and the sea surface observed near nadir is affected by several error sources when the signal passes the atmosphere. Additionally, several tidal effects are involved in measuring the sea level. Therefore, the following atmospheric and geophysical corrections were used:

$$cor = \Delta h_{iono} + \Delta h_{dry} + \Delta h_{wet} + \Delta h_{ssb} + \sum h_t + h_a + h_f, \tag{1}$$

where the meanings of corrections are ionospheric correction Δh_{iono}, dry and wet tropospheric corrections Δh_{dry} and Δh_{wet}, sea state bias correction Δh_{ssb}, sum of tide heights $\sum h_t$ (solid earth, geocentric ocean and geocentric pole tide height), inverted barometer height correction h_a and high frequency fluctuations of the sea surface topography correction h_f, respectively.

The corrected range between the satellite and the sea level was calculated:

$$R_{cor} = R + cor, \tag{2}$$

where R is the directly measured distance or pseudorange between the satellite and the sea level (Figure 3). Sea surface height above the ellipsoid (SSH_{alt}) based on the off-centre-of-gravity (OCOG) retracker, which is empirically fit various types of waveforms [21; 22], was calculated:

$$SSH_{alt} = h_{sat} - R_{cor}, \tag{3}$$

where h_{sat} is satellite height above ellipsoid (WGS84), which can be calculated using satellite ephemeris.

SSH_{alt} values were calculated for all transects (Figure 2) in the period from 1 January 2019 to 1 November 2019, equivalent to 10-11 cycles for each pass.
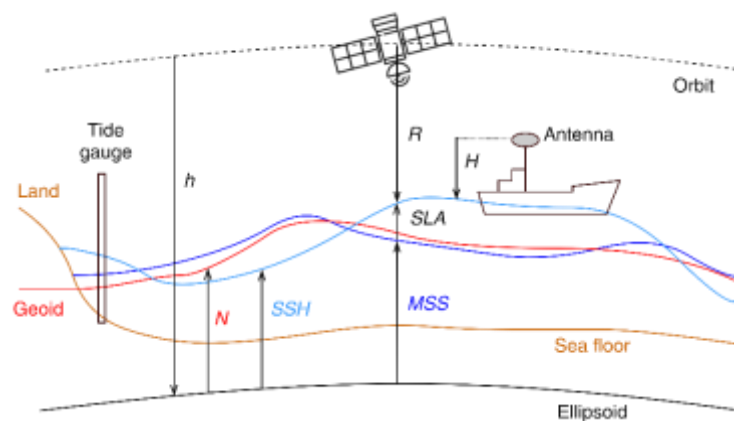

Figure 3. Schematic plot of the relationship between the sea surface height measured by satellite altimetry, tide gauge and GNSS on the vessel. Abbreviations meaning: *SSH* – sea surface height, *MSS* – mean sea surface, *SLA* – sea-level anomaly, *h* – ellipsoidal height, *N* – undulation of the geoid.

The SAR mode of Sentinel-3 effectively reduces land-induced contamination in the radar signal by increasing the spatial resolution along track. However, the problem still exists when the satellite azimuth direction and the coastline are not perpendicular. Therefore, Sentinel-3 measurements within 2 km of the shoreline were removed in order to reduce potential noisy data, as demonstrated by the blue points appearing between the grey and red lines in Figure 4. Normally, the differences (ΔSSH) between the sea-level anomaly corrected geoid model (SSH_{geoid}) and satellite altimetry (SSH_{alt}) remained within 0.5-1 m. However, some ΔSSH outliers could be up to 2 m or more on open water due to reflections from small islets or vessels, which is known as the 'hooking effect' in off-nadir measurements.
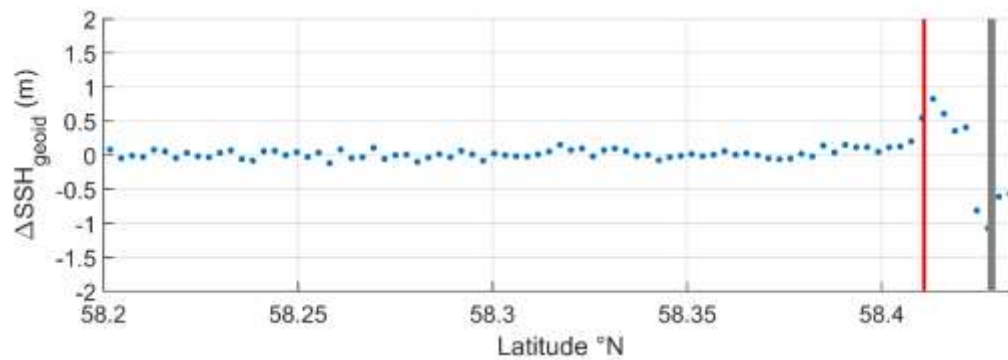

Figure 4. An example of the effect of the coastal zone on Sentinel-3 data. S3A pass 093 sea-level height was compared with the sea-level anomaly corrected geoid height (ΔSSH_{geoid}, Eq. 5) in the Gulf of Riga. The grey and red lines indicate the coast and the distance (2 km) from the coast, respectively.

2.5. In Situ Data

The Estonian coastline has a dense **tide gauge network**, from which 21 stations were selected for the study (Figure 2). Among them, 13 stations are managed by the Estonian Environmental Agency (EEA) and 8 stations are operated by the Department of Marine Systems (MSI) of Tallinn University of Technology. All of these tide gauges are equipped with pressure sensors and have operated for more than ten years already [19]. In 2017-2018, the automatic tide gauges as well as tide gauge rods were reconnected to the national levelling network. Today, the automatic tide gauges record the hourly sea-level height in the Estonian height system EH2000, which is a national realisation of the European Vertical Reference System EVRS [23].

The tide gauge data were used to estimate sea-level anomaly along each altimetry track. Sea-level anomaly from tide gauges (SLA_{TG}) was calculated from the four tide gauge records nearest to the satellite track at the time of the satellite overpass. The average of SLA_{TG} was used to correct the geoid height (N) from the EST-GEOID2017 model above the ellipsoid GRS80. The geoid-based sea surface height (SSH_{geoid}) at each high-frequency Sentinel-3 footprint can thus be presented as:

$$SSH_{geoid} = SLA_{TG} + N. \tag{4}$$

For Sentinel-3 validation, the difference between altimetry-based sea surface height (SSH_{alt}) and geoid-based sea surface height (SSH_{geoid}) was calculated using the following equation:

$$\Delta SSH_{geoid} = SSH_{alt} - SSH_{geoid}. \tag{5}$$

Residual difference ΔSSH_{geoid} was further analysed. The ΔSSH_{geoid} residuals larger than 2.5 standard deviation were considered outliers. Residuals were plotted against distance from the coast (Figure 4). Correlation plots between SSH_{alt} and SSH_{geoid} were compiled as well.

In addition, **GNSS kinematic measurements** on the vessels were used to validate SSH_{alt} over the study sites. Multiple-frequency Trimble R8s and Trimble R4-3 receivers were mounted on top of the vessel (Figure 5b). Antenna reference points were connected to the sea level using a total station (Figure 5a). Two antennas were used to eliminate the risks when one receiver stops working and also to filter out vessel fluctuations [24, 25]. Measurements were carried out on the same day of the satellite overpass

and the weather was calm during all measurements (Table 1). GNSS measurements were recorded at 2-second intervals along the altimetry tracks (see Figure 2). The first data quality control was performed on board the vessel with the program TEQC [26]. The GNSS base stations data from the Estonian Permanent GNSS Network ESTPOS [27] and the Trimble Business Centre software were used for kinematic data processing in double difference mode. The International Geodetic Service (IGS) precise ephemeris and absolute antenna calibration data were used. First, both receiver data were processed separately and sea-level heights above the ellipsoid from two receivers were compared. When the difference between the sea-level heights from two receivers on the same time tag was larger than ±10 cm, the measurement was excluded from further processing. Cleaned heights from two receivers on the same time tag were averaged. Next, the temporally moving-averaged sea-level height was calculated in order to smooth out the fluctuations of the vessels. The window size for the moving average filter was selected based on the velocity of the vessel and the GNSS data rate (2 s) in order to obtain window size, which is close to the altimeter along-track resolution (300 m). For example, if the vessel's velocity was 10 m/s and the GNSS sample rate was 2 s, moving average window 15 was chosen, since 15 x 2 x 10 = 300 m. Spatially moving-averaged GNSS sea surface heights (SSH_{GNSS}) were compared with SSH_{alt} for altimetry validation:

$$\Delta SSH_{GNSS} = SSH_{alt} - SSH_{GNSS}. \tag{6}$$

(a)   (b)

Figure 5. Research vessel SALME **(a)** and the GNSS receivers on top of the wheelhouse **(b)**. The total station used to connect the GNSS antenna's reference point with sea level.

Table 1. General parameters of the GNSS kinematic measurements.

Waterbody	Gulf of Finland	Gulf of Riga	Lake Peipus	Lake Võrtsjärv
Date	25.04.2019	20.06.2019	19.06.2019	13.07.2019
Weather conditions	Light wind, waves up to 1 m	Calm, no waves	Calm, no waves	Calm, no waves
Profile length (km)	25	54	33	10
Vessel				

In addition, a **pressure sensor-based buoy** (Figure 6) was mounted on the seafloor of the Gulf of Riga (Figure 2) for five months (June-November 2019). The crossing point of the S3A pass 186 and 397 tracks (58°07'12''N and 23°32'06''E) was chosen for the buoy location. Sea-level data were recorded by buoy at 5-minute intervals. The buoy's records were connected to ellipsoidal heights. For this, the water

column height above the sensor was measured by tape and it was connected with the GNSS height during mounting.
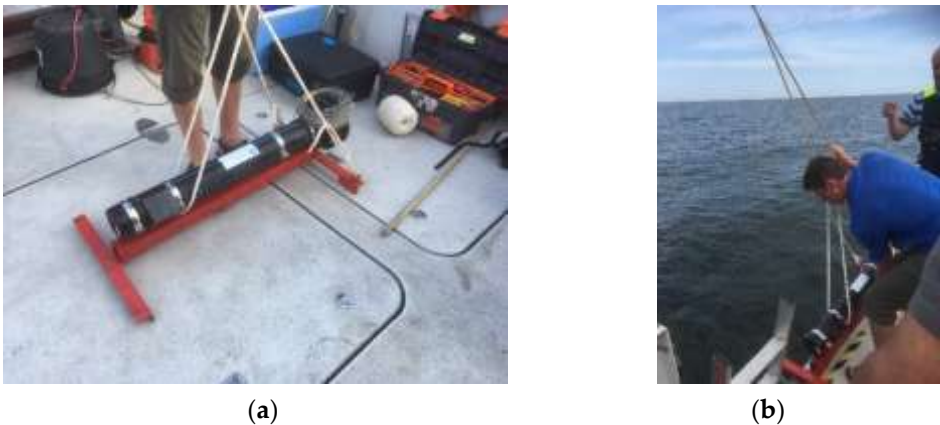

| (a) | (b) |

Figure 6. Pressure sensor-based buoy **(a)** and its mounting **(b)** in the Gulf of Riga on 20 June 2019.

2.6. Copernicus Marine Environment Monitoring Service (CMEMS) data products

One of the purposes of this study was to compare the accuracy of CMEMS Level-3 (L3) along-track altimetry products (SLA_{L3}) [28] and NEMO reanalysis model (SLA_{NEMO}) [29] outcomes against the sea-level anomaly data from coastal tide gauge stations (SLA_{TG}). The CMEMS Baltic Sea Physical Reanalysis product provides a physical reanalysis for the entire Baltic Sea area. It is produced using the ice-ocean model NEMO-Nordic [29]. The reported mean correlation between SLA_{TG} and SLA_{NEMO} for the entire Baltic Sea is 0.95 with an RMSE of 7 cm, with lower values in highly dynamic marine areas [30].

The analysed *SLA* data covered the period from 2014 to 2017 when the sea-level measurements of all methods were available. The SLA_{L3} altimetry data was collected only from the altimeters that were active in 2019 (Table 2). An overview of tide gauges is given in Altimetry SLAL3 measurements were collected at a maximum distance of 10 km offshore from the listed gauges, and the maximum time difference between SLA_{TG} and SLA_{L3} measurements was one hour. For the NEMO, SLA_{NEMO} at the closest grid point to the station within an hour's time difference was extracted. SLA data from all seasons (including winters with ice cover) was used in the comparison. Finally, a selection was made from all three sources to match the measurements by time. The number of common, collocated measurements was 625.

A separate comparison was carried out with the data from the buoy in the Gulf of Riga (cf. green circle on Figure 2) to measure the accuracy of SLA_{L3} along-track data as well as the reanalysis model outcomes. The data was collected using the same scheme as that of the other stations described above, and the final analysis consisted of 33 unique data points in all three sources.

Data analysis results were presented as standard descriptive statistics: Pearson correlation coefficient (*r*), Root Mean Square Error (RMSE) and Mean Error (ME). The statistics were calculated between SLA values since the accurate translation of modelled water levels into a common reference surface is an as yet unresolved technical issue [31].

Table 3.

Table 2. Overview of the satellite altimetry missions used.

Mission	Period	Measurements
Saral/Altika	13.01.2014-31.12.2017	167
CryoSat-2	05.01.2014-31.12.2017	225
HY2A	24.04.2014-31.12.2017	111
Jason-2	09.01.2014-31.12.2017	50

Jason-3	30.05.2016-31.12.2017	24
Sentinel-3A	01.07.2016-31.12.2017	48

Altimetry SLA_{L3} measurements were collected at a maximum distance of 10 km offshore from the listed gauges, and the maximum time difference between SLA_{TG} and SLA_{L3} measurements was one hour. For the NEMO, SLA_{NEMO} at the closest grid point to the station within an hour's time difference was extracted. SLA data from all seasons (including winters with ice cover) was used in the comparison. Finally, a selection was made from all three sources to match the measurements by time. The number of common, collocated measurements was 625.

A separate comparison was carried out with the data from the buoy in the Gulf of Riga (cf. green circle on Figure 2) to measure the accuracy of SLA_{L3} along-track data as well as the reanalysis model outcomes. The data was collected using the same scheme as that of the other stations described above, and the final analysis consisted of 33 unique data points in all three sources.

Data analysis results were presented as standard descriptive statistics: Pearson correlation coefficient (r), Root Mean Square Error (RMSE) and Mean Error (ME). The statistics were calculated between SLA values since the accurate translation of modelled water levels into a common reference surface is an as yet unresolved technical issue [31].

Table 3. Overview of tide gauges (Figure 2) used for comparison with CMEMS products. Comparison results (r and RMSE) between SLA_{TG}, SLA_{L3} and SLA_{NEMO} are shown in the last four columns (cf. chapter 3.4).

Station no.	Station name	No. of common measurements	SLA_{TG} vs SLA_{L3} r	SLA_{TG} vs SLA_{L3} RMSE	SLA_{TG} vs SLA_{NEMO} r	SLA_{TG} vs SLA_{NEMO} RMSE
1	Dirhami	116	0.83	0.17	0.93	0.26
2	Kunda	22	0.88	0.22	0.92	0.29
3	Narva-Jõesuu	32	0.71	0.35	0.97	0.29
4	Loksa	7	0.82	0.14	0.83	0.21
5	Pirita	5	0.90	0.09	0.94	0.21
6	Paldiski	5	0.79	0.17	0.87	0.26
7	Ristna	73	0.86	0.17	0.92	0.30
8	Heltermaa	20	0.88	0.09	0.83	0.27
9	Virtsu	19	0.81	0.15	0.90	0.26
10	Roomassaare	18	0.73	0.18	0.89	0.27
11	Ruhnu	82	0.86	0.20	0.92	0.31
12	Häädemeeste	41	0.76	0.19	0.88	0.30
13	Pärnu	8	0.86	0.17	0.97	0.27
14	Muuga	15	0.80	0.17	0.83	0.27
15	Tallinna Sadam	4	0.97	0.08	0.95	0.24
16	Paldiski (MSI)	15	0.83	0.23	0.88	0.31
17	Lehtma	82	0.85	0.14	0.93	0.21
18	Heltermaa (MSI)	21	0.85	0.10	0.87	0.24
19	Triigi	5	0.77	0.09	0.91	0.22
20	Virtsu	17	0.82	0.23	0.91	0.33
21	Rohuküla (MSI)	18	0.94	0.17	0.96	0.25
	Total/average	*625*	*0.80*	*0.19*	*0.91*	*0.27*

3. Results and Discussion

3.1. Sentinel-3 Level-2 validation with GNSS campaigns

The statistics of the residuals from the Eq. (6) along altimetry tracks are presented in Table 4. According to the results in multiple locations, the two datasets in the Baltic Sea correspond better than those of inland cases; the mean (MEAN) and standard deviation (STD) were 0.11 ±0.08 m and 0.14 ±0.05 m in the Gulf of Finland and the Gulf of Riga, respectively. These results also match well with the validation by the geoid model for S3B pass 625 in the Gulf of Finland on 25 April 2019 (0.11 ±0.06 m) (Figure 7) and for S3A pass 186 in the Gulf of Riga on 20 June 2019 (0.09 ±0.05 m) (Figure 8). In Lake Peipus and Lake Võrtsjärv, the MEAN and STD were 0.16 ±0.13 m and 0.31 ±0.39 m, respectively. Again, these GNSS validation results agree with the validation results using the geoid model, showing a discrepancy of 0.15 ±0.14 m and 0.28 ±0.30 m for the Lake Peipus on 19 June 2019 and for Lake Võrtsjärv on 13 July 2019, respectively (Figure 9). Compared with marine conditions, the worse performance on the lakes could be attributed to several factors, such as vegetation coverage near shore and the hooking effect from the surrounding land [32]. It is also arguably due to the fact that the geophysical corrections (Eq. 1) for continental waters are not as accurate as for the open sea [33].

The other error sources for the determination of ΔSSH_{GNSS} are: (i) errors in the determination of the GNSS antenna height from the water level; the uncertainty of the sea surface height from the GNSS antenna is at least ±0.020 m and it is possible that the GNSS antenna connection to the water level could also cause a systematic shift; and (ii) the accuracy of the GNSS solution itself. Multiple-frequency Trimble R8s and Trimble R4-3 receivers were used for the GNSS kinematic measurements on the boat but the vertical uncertainty could be ±0.015 m + 1 ppm RMS according to the manufacturer's specification. It is also noted that the mean ΔSSH_{GNSS} is biased in all waterbodies, especially in Lake Võrtsjärv.

Table 4. Statistics of differences between the sea surface height (ΔSSH_{GNSS}) derived from GNSS measurements (SSH_{GNSS}) and sea surface height derived from altimetry (SSH_{alt}) according to the Eq. (6).

Statistics	Gulf of Finland	Gulf of Riga	Lake Peipus	Lake Võrtsjärv
MEAN (m)	0.11	0.14	0.16	0.31
STD (m)	0.08	0.05	0.13	0.39
RMSE (m)	0.13	0.15	0.21	0.49
MIN (m)	-0.11	0.00	-0.33	-0.45
MAX (m)	0.29	0.27	0.38	0.74

3.2. Sentinel-3 validation with the SLA-corrected EST-GEOID2017

We studied the waterbodies separately for validation with the geoid model. Two transects were chosen for the Gulf of Finland (Figure 2) and the residual of differences for S3A and S3B (ΔSSH_{geoid}, Eq. 5) are presented in Figure 7. The mean ΔSSH_{geoid} was calculated for each 25-km-long transect when the satellite passed over the gulf. The time difference between SA3 and S3B overpasses is two days. It is observed that the validation results and trends for both passes (S3A_186 and S3B_625) are very similar in the Gulf of Finland, which implies a similar accuracy level for both missions. The average ΔSSH_{geoid} for S3A and S3B was 0.02 ±0.08 m. Note that there is no ΔSSH value for S3B for May 2019 (Figure 7, cycle 25) because the ΔSSH_{geoid} at 0.31 ±0.55 m in this cycle is clearly an outlier. Such a big residual difference could have been caused by a local wind-driven water pile up against the coast. After removing ΔSSH_{geoid} from cycle 25, an average residual difference of 0.01 ±0.06 m was obtained for the Gulf of Finland (Table 5).
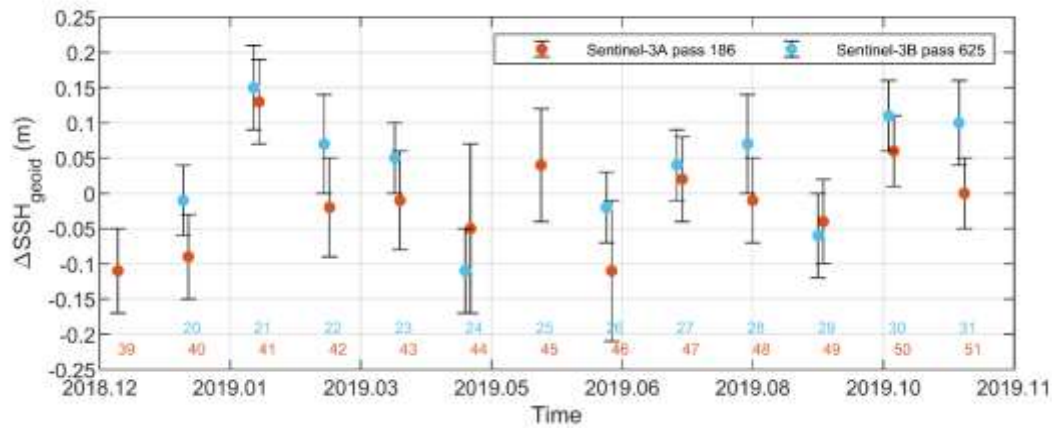
Figure 7. Residual differences (ΔSSH_{geoid}) between the sea surface height of Sentinel-3 (SSH_{alt}) and the geoid-based sea surface height (SSH_{geoid}) in the Gulf of Finland. The zero line denotes the reference SSH_{geoid}. Coloured numbers indicate the corresponding cycle number for each satellite.
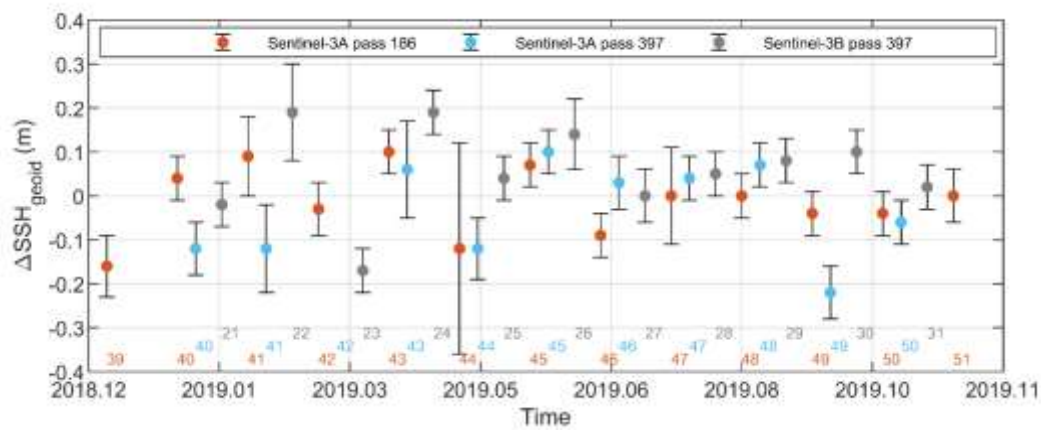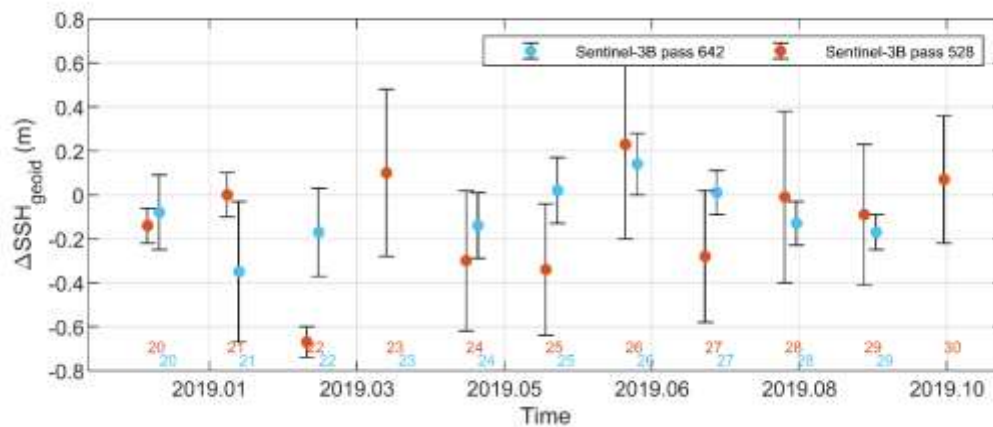

Figure 8. Residual differences (ΔSSH_{geoid}) between the sea surface height of Sentinel-3 (SSH_{alt}) and the geoid-based sea surface height (SSH_{geoid}) in the Gulf of Riga. The zero line denotes the reference SSH_{geoid}. Coloured numbers indicate the corresponding cycle number for each satellite.

Table 5. Statistics of differences between the sea surface heights derived from altimetry (SSH_{alt}) and geoid-based sea surface height (SSH_{geoid}) according to the Eq. (5).

Statistics	Gulf of Finland	Gulf of Riga	Lake Peipus	Lake Võrtsjärv
MEAN (m)	0.01	0.00	0.14	0.13
STD (m)	0.06	0.07	0.16	0.27
RMSE (m)	0.07	0.10	0.23	0.27
MIN (m)	-0.32	-0.98	-0.56	-1.13
MAX (m)	0.33	0.58	0.98	0.78

Three transects were chosen for comparison in the Gulf of Riga: S3A pass 186, S3A pass 397 and S3B pass 397 (Figure 2). The results of S3A and S3B fit quite well in the Gulf of Riga (Figure 8). S3A 186 showed a better fit due to the shorter transect (54 km). Larger deviations were observed in winter from December to April when stormy weather conditions prevailed. Wind set-up near the coast is proportional to tangential wind speed component squared and can reach up to *ca* 1 m in certain Estonian coastal locations during strong storms [34]. The average residual differences between the sea surface height of Sentinel-3 (SSH_{alt}) and geoid-based sea surface height (SSH_{geoid}) was 0.01 ±0.07

m. After removing an outlier (S3A pass 397 cyc 25 (11.03.2019) ΔSSH_{geoid} = 0.410 ±0.600 m), the average residual difference for the Gulf of Riga is 0.00 ±0.07 m (Table 5).

The validation results for the lakes show much larger discrepancies compared with the results in the gulfs (Figure 9). The main reasons for this are the size of the water body and the distance of the track from the coastline. In winter, the results are also affected by the sea/lake ice. In February and March, both lakes were covered by ice and snow up to 0.4 m thick and hummock ice occurred in the coastal areas as well. Thus, the average residual differences between the sea surface height of Sentinel-3 (SSH_{alt}) and geoid-based sea surface height (SSH_{geoid}) for Sentinel-3B in Lake Peipus and Lake Võrtsjärv were 0.14 ±0.16 m and 0.13 ±0.27 m, respectively (Table 5).

Figure 9. Residual differences (ΔSSH_{geoid}) between the sea surface height of Sentinel-3 (SSH_{alt}) and geoid-based water surface height (SSH_{geoid}) in Lake Peipus (blue dots) and Lake Võrtsjärv (red dots). The zero line denotes the reference SSH_{geoid}. Coloured numbers indicate the cycle's number.

3.3. Sentinel-3 validation with buoy data in the Gulf of Riga

The buoy placed on the bottom of the Gulf of Riga was collecting sea surface height data (SSH_{buoy}) from June 2019 until November 2019. During this period, satellite tracks S3A_186 and S3A_397 passed the buoy six and five times, respectively. For the validation, the mean SSH_{alt} was calculated using the altimetry data within a radius of 5 km from the buoy. It was compared with the buoy SSH_{buoy} for the same time, cf. Figure 10. According to the results, the agreement between the two datasets is very good (Pearson correlation coefficients r for S3A_186 and S3A_397 were 0.88 and 0.95, respectively). The mean residual differences (ΔSSH) and STD were 0.05 ±0.06 and -0.03 ±0.10 m for S3A_186 and S3A_397, respectively.
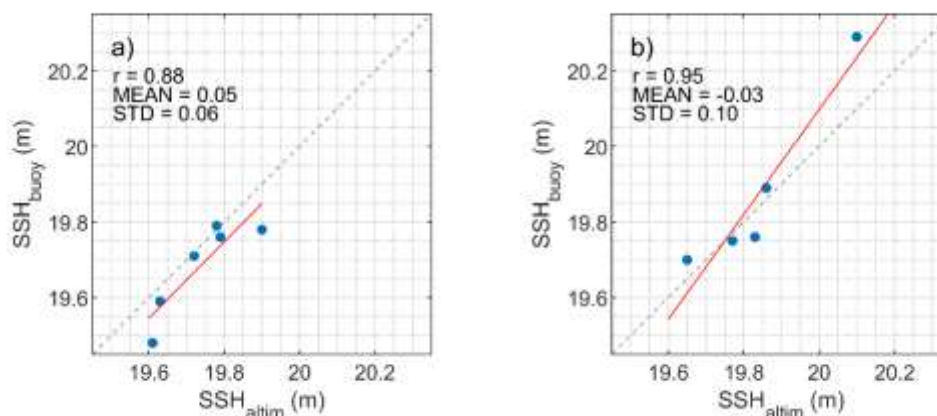

Figure 10. Comparison of Sentinel-3 (SSH_{alt}) and buoy (SSH_{buoy}) sea surface heights on **(a)** S3A pass 186 and **(b)** S3A pass 397 in the Gulf of Riga. Red line is the linear regression between the two datasets.

3.4. SLA_{L3} and SLA_{NEMO} comparison with in situ SLA_{TG} measurements

The CMEMS SLA_{L3} along-track altimetry data comparison with SLA_{TG} measurements yielded accurate results with the Pearson correlation coefficient $r = 0.80$ for all stations in sum (Altimetry SLAL3 measurements were collected at a maximum distance of 10 km offshore from the listed gauges, and the maximum time difference between SLA_{TG} and SLA_{L3} measurements was one hour. For the NEMO, SLA_{NEMO} at the closest grid point to the station within an hour's time difference was extracted. SLA data from all seasons (including winters with ice cover) was used in the comparison. Finally, a selection was made from all three sources to match the measurements by time. The number of common, collocated measurements was 625.

A separate comparison was carried out with the data from the buoy in the Gulf of Riga (cf. green circle on Figure 2) to measure the accuracy of SLA_{L3} along-track data as well as the reanalysis model outcomes. The data was collected using the same scheme as that of the other stations described above, and the final analysis consisted of 33 unique data points in all three sources.

Data analysis results were presented as standard descriptive statistics: Pearson correlation coefficient (r), Root Mean Square Error (RMSE) and Mean Error (ME). The statistics were calculated between SLA values since the accurate translation of modelled water levels into a common reference surface is an as yet unresolved technical issue [31].

Table 3, Figure 11a). The RMSE for all stations together was 0.19 m, the mean error was 0.12 m and the STD between SLA_{TG} and SLA_{L3} was 0.14 m. These results are similar to previous findings for the area even though the RMSE is larger [35]. The correlation between SLA_{TG} and SLA_{NEMO} is higher ($r = 0.91$, Figure 11b, Altimetry SLAL3 measurements were collected at a maximum distance of 10 km offshore from the listed gauges, and the maximum time difference between SLA_{TG} and SLA_{L3} measurements was one hour. For the NEMO, SLA_{NEMO} at the closest grid point to the station within an hour's time difference was extracted. SLA data from all seasons (including winters with ice cover) was used in the comparison. Finally, a selection was made from all three sources to match the measurements by time. The number of common, collocated measurements was 625.

Table 3). However, the RMSE and mean error are much higher at 0.27 m and 0.26 m, respectively, which indicates a bias in the model fields. Standard deviation on the other hand was 0.10 m. The comparison with Narva-Jõesuu station (tide gauge number 3 in Figure 2, Altimetry SLAL3 measurements were collected at a maximum distance of 10 km offshore from the listed gauges, and the maximum time difference between SLA_{TG} and SLA_{L3} measurements was one hour. For the NEMO, SLA_{NEMO} at the closest grid point to the station within an hour's time difference was extracted. SLA data from all seasons (including winters with ice cover) was used in the comparison. Finally, a selection was made from all three sources to match the measurements by time. The number of common, collocated measurements was 625.

Table 3) shows the worst performance regarding its low correlation and high RMSE (0.35 m) and mean error (0.30 m). A closer look at the data shows that *ca* 30% of the data were collected in winter, which may be one of the reasons the satellite results are underestimated. In addition, the exact measurement point in Narva-Jõesuu is at the mouth of Narva River. The location may also hinder the quality of *in situ* measurements, as the dynamics of the river itself are not recorded in the satellite results within a 10 km radius.
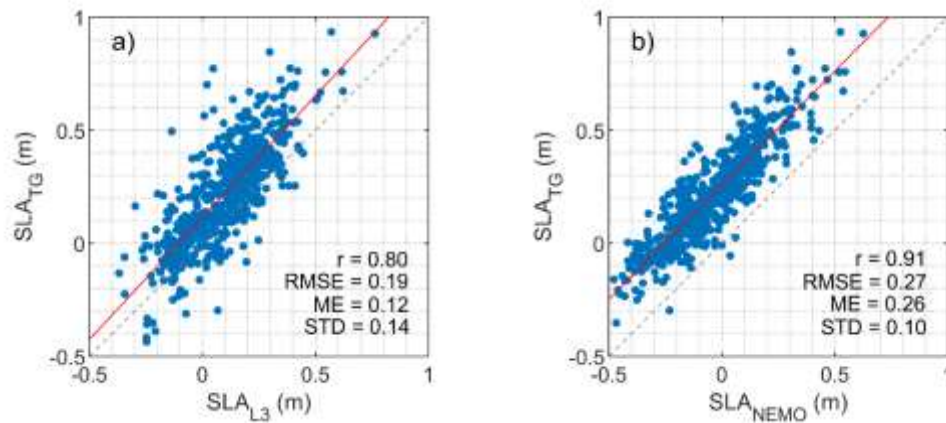
Figure 11. Comparison of tide gauge-based sea-level measurements (SLA_{TG}) with **(a)** altimetry CMEMS Level 3 sea-level anomaly (SLA_{L3}) and **(b)** NEMO reanalysis model (SLA_{NEMO}), respectively. Red line is the linear regression between the two datasets.

In Figure 12, a comparison of the SLA_{buoy} data from the Gulf of Riga open sea station (green circle in Figure 2) with SLA_{L3} data and SLA_{NEMO} data is shown. Surprisingly, along-track SLA accuracy gained little to no improvement compared with the results of coastal measurements, whereas NEMO reanalysis model outcomes improved significantly on the open sea. This suggests that the NEMO reanalysis fields represent sea-level variations on the open sea with high accuracy, while in the coastal region where the sea level is influenced by various processes and factors (shallow areas, coastal effects, waves, etc.), the model reanalysis data loses some of its accuracy.
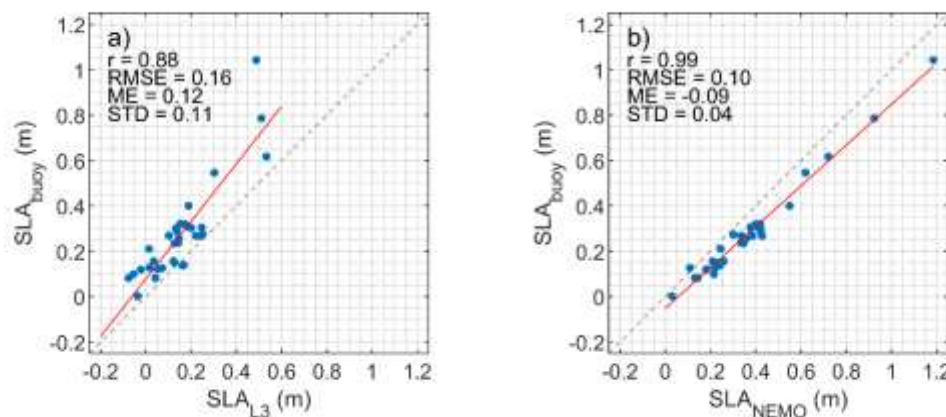

Figure 12. Comparison of buoy-based sea-level measurements (SLA_{buoy}) with **(a)** altimetry CMEMS Level 3 sea-level anomaly (SLA_{L3}) and **(b)** NEMO reanalysis model (SLA_{NEMO}) in the Gulf of Riga (green circle in Figure 2). Red line is the linear regression between the two datasets.

The good correlation between the SLA measurements and the SLA_{NEMO} (Figure 11b, Figure 12b) proves that the reanalysis model NEMO calculates water level dynamics very well. This is in accordance with the accuracy of the CMEMS reanalysis product in the relatively dynamic coastal sea area [30]. However, the RMSE in the current study is even larger than in the model product quality analysis (7 cm) [30]. The higher RMSE value is clearly influenced by the bias (ME = 0.26 m). The large

RMSE can be seen on the frequency distribution of water level anomalies in Figure 13. The maximum frequency distribution of model results is around zero water level, whereas it is around +0.2 m for SLA_{TG} measurements. However, the small STD (±0.10) shows the good fit of the model with the observations when bias is removed and is comparable with the RMSE found in [30].

The STD between SLA_{TG} measurements and SLA_{L3} (Figure 11a) is higher than that of model outcome comparison (Figure 11b). This could be explained by *(i)* land contamination which exists in altimetry results, *(ii)* altimetry processing in general, *(iii)* tide gauge measurement errors, or *(iv)* the fact that SLA_{L3} data were collected at a maximum distance of 10 km from the tide gauge station and even by the time difference between compared measurements. The reasoning above is confirmed by a comparison of SLA_{L3} with SLA_{buoy} measurements from the buoy in the Gulf of Riga (Figure 12). Even though there should be very little land influence if any on the altimeters that measured over the station, a distinguishable offset is still present between the remotely sensed and modelled sea level (Figure 12a and b). This indicates possible errors in altimetry processing. However, the smaller ME, RMSE and STD on Figure 13b compared with 12b indicate that the performance of the NEMO model is better on the open sea compared with the coastal Baltic Sea.

In general, validation of altimetry products with tide gauge data in the coastal area, although constantly improving, still remains a challenge [31, 36]. This is because of various coastal effects as well as possible geoid connection issues. Moreover, a mismatch of characteristic (temporal and spatial) scales inevitably exists when sampling the SSH variability with different methods, such as coastal tide gauges, relatively coarse-gridded models and remote sensing products.
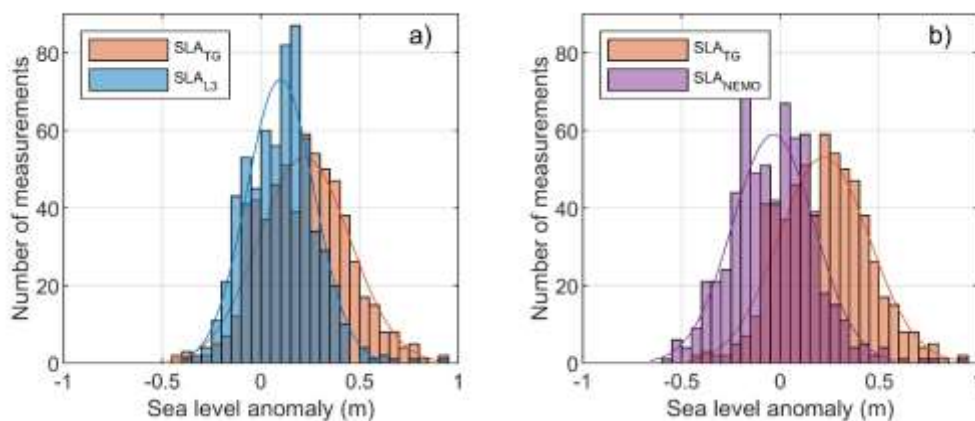

Figure 13. Sea-level anomaly frequency distribution calculated with a bin size of 0.05 m for **(a)** SLA_{TG} and SLA_{L3} and **(b)** SLA_{TG} and SLA_{NEMO} in the Baltic Sea.

4. Conclusions

This study discussed the quality of the Sentinel-3A/B Level-2 product and the Copernicus Marine Environment Monitoring Service (CMEMS) Level-3 product. To validate the Level-2 product, the SSH from altimetry (SSH_{alt}) in Estonian coastal waters (Gulf of Finland and Gulf of Riga) and larger lakes (Lake Peipus and Lake Võrtsjärv) was compared with the SSH obtained from GNSS (SSH_{GNSS}) and buoy (SSH_{buoy}) measurements, *in situ* coastal tide gauges and national geoid model EST-GEOID2017 (SSH_{geoid}). In addition, to validate the along-track Level-3 product (SLA_{L3}) and NEMO reanalysis outcomes (SLA_{NEMO}) from the CMEMS database, the water levels were compared with *in situ* measurements at 21 Estonian coastal tide gauge stations. The comparison was made with data from six satellites from 2014 to 2017.

The validation results of the Sentinel-3 Level-2 product showed that the altimetry accuracy is much higher (~3x) on the open sea than on lakes. The average difference between SSH_{alt} and SSH_{geoid} (residual difference ΔSSH, Eq. 5) was 0.07-0.10 m in the Gulf of Finland and the Gulf of Riga. The corresponding numbers were 0.23 and 0.27 m in Lakes Peipsi and Võrtsjärv, respectively. Based on the average residual differences, it was noted that the altimetry SSH values in inland waters were systematically shifted: SSH_{alt} was 0.14 m and 0.13 m higher than SSH_{geoid} values in Lake Peipus and

Lake Võrtsjärv, respectively. In the coastal waters, positive and negative residual differences were more equally distributed, i.e. average residual differences were close to zero. Validation with GNSS showed good consistency with validation using the geoid model. The best fit with the altimetry height was found using buoy measurements in the Gulf of Riga (average difference 0.01 ±0.09 m). In summary, considering all validation methods, our results show that satellite altimetry can determine the height of the water level in Estonian coastal areas with an average accuracy of 0.08 ±0.07 m and in inland waters 0.20 ±0.26 m.

The Level-3 along-track altimetry products from six active altimeter missions and the modelled results from the NEMO reanalysis product (available at CMEMS database) were compared with *in situ* tide gauge measurements between 2014 and 2017. The sea-level anomaly comparison between the three data sources was carried out with concurrent measurements at 21 stations around the Estonian coast (from 2014-2017) and a buoy station in the open part of the Gulf of Riga (in 2019).

The validation of the CMEMS Level-3 data shows that the altimeter water level data and Sentinel-3A/B Level-2 product have similar accuracy. The residual difference between the NEMO reanalysis model and the satellite data was approximately twofold near the coast compared with the open sea. The Pearson correlation coefficient on the other hand was better for the SLA_{NEMO} than the SLA_{L3} data near the coast. The mean correlation between the NEMO fields and the *in-situ* measurements was 0.91 and the mean difference was 0.26 m. The respective statistics between the satellite and the *in-situ* measurements were 0.80 and 0.12 m. This shows that satellite measurements near the coast have, on average, a mean error twice as low as that of the NEMO model. However, the offshore water level data from the NEMO model is very accurate ($r = 0.99$, mean error -9 cm), while the satellite sea level remains on a similar accuracy level as in the coastal areas.

Conflicts of Interest: The authors declare no conflict of interest.

References

1. Shum, C.K.; Ries, J.C.; Tapley, B.D. (1995). The accuracy and applications of satellite altimetry. *Geophysical Journal International* 1995, 121(2), 321-336.

2. Míguez, B.M.; Testut, L.; Wöppelmann, G. Performance of modern tide gauges: towards mm-level accuracy. *Scientia Marina* 2012, 76(S1), 221-228, doi: 10.3989/scimar.03618.18A.

3. Ollivier, A.; Faugere, Y.; Picot, N.; Ablain, M.; Femenias, P.; Benveniste, J. Envisat Ocean altimeter becoming relevant for mean sea level trend studies. *Marine Geodesy* 2012, 35(1), 118–136, doi: 10.1080/01490419.2012.721632.

4. Prandi, P.; Philipps, S.; Pignot, V.; Picot, N. SARAL/AltiKa global statistical assessment and cross-calibration with Jason-2. *Marine Geodesy* 2015, 38(1), 297–312, doi: 10.1080/01490419.2014.995840.

5. Raney, R.K. The delay/Doppler radar altimeter. *IEEE Transactions on Geoscience and Remote Sensing* 1998, 36(5), 1578-1588, doi: 10.1109/36.718861.

6. Vignudelli, S.; Birol, F.; Benveniste, J.; Fu, L.-L.; Picot, N.; Raynal, M.; Roinard, H. Satellite Altimetry Measurements of Sea Level in the Coastal Zone. *Surveys in Geophysics* 2019, 40(6), 1319–1349, doi: 10.1007/s10712-019-09569-1.

7. Wingham, D.J.; Francis, C.R.; Baker, S.; Bouzinac, C.; Cullen, R.; de Chateau-Thierry, P.; Laxon, S. W.; Mallow, U.; Mavrocordatos, C.; Phalippou, L.; Ratier, G.; Rey, L.; Rostan, F.; Viau, P.; Wallis, D. CryoSat: a mission to determine the fluctuations in earth's land and marine ice fields. *Advances in Space Research* 2006, 37(4), 841–871, doi: 10.1016/j.asr.2005.07.027.

8. Santos-Ferreira, A.M.; Silva, J.C.B.; Magalhães, J.M. SAR Mode Altimetry Observations of Internal Solitary Waves in the Tropical Ocean Part 1: Case Studies, *Remote Sensing* 2018, 10(4), 644, doi: 10.3390/rs10040644

9. Shu, S.; Liu, H.; Beck, R.A.; Frappart, F.; Korhonen, J.; Xu, M.; Yang, B.; Hinkel, K.M.; Huang, Y.; Yu, B. Analysis of Sentinel-3 SAR altimetry waveform retracking algorithms for deriving temporally consistent water levels over ice-covered lakes. *Remote Sensing of Environment* 2020, 239, doi: 10.1016/j.rse.2020.111643.

10. Birgiel, E.; Ellmann, A.; Delpeche-Ellmann, N. Examining the Performance of the Sentinel-3 Coastal Altimetry in the Baltic Sea Using a Regional High-Resolution Geoid Model. 2018 Baltic Geodetic Congress (BGC Geomatics), pp. 196-201, doi: 10.1109/BGC-Geomatics.2018.00043.

11. Birkett, C.; Reynolds, C.; Beckley, B.D. From research to operations: the USDA global reservoir and lake monitor. In: S. Vignudelli, A.G. Kostianoy, P. Cipollini, J. Benveniste (Eds.), Coastal Altimetry, Springer Berlin Heidelberg, Berlin, Heidelberg 2011, pp. 19-50.

12. Ruiz Etcheverry, L.A.; Saraceno, M; Piola, A.R.; Valladeau, G.; Möller, O.O. A comparison of the annual cycle of sea level in coastal areas from gridded satellite altimetry and tide gauges. *Continental Shelf Research* 2015, 92, 87-97, doi: 10.1016/j.csr.2014.10.006.

13. Ardalan, A.A.; Jazireeyan, I.; Abdi, N.; Rezvani, M.H. Evaluation of SARAL/AltiKa performance using GNSS/IMU equipped buoy in Sajafi, Imam Hassan and Kangan Ports. *Advances in Space Research* 2018, 61(6), 1537-1545, doi: 10.1016/j.asr.2018.01.001.

14. Bonnefond, P.; Exertier, P.; Laurain, O.; Ménard, Y.; Orsoni, A.; Jeansou, E.; Haines, B.J.; Kubitschek, D.G.; Born, G. Leveling the Sea Surface Using a GPS-Catamaran Special Issue: Jason-1 Calibration/Validation. *Marine Geodesy* 2003, 26(3-4), 319-334, doi: 10.1080/714044524.

15. Medvedev, I.P.; Rabinovich, A.B.; Kulikov, E.A. Tidal Oscillations in the Baltic Sea. *Oceanology* 2013, 53(5), 526-538, doi: 10.1134/S0001437013050123.

16. Mayer-Guerr, T. The combined satellite gravity field model GOCO05s. In: EGU general assembly conference abstracts 2015, 17.

17. Ellmann, A.; Märdla, S.; Oja, T. The 5 mm geoid model for Estonia computed by the least squares modified Stokes's formula. *Survey Review* 2020, 52(373), 352-371, doi: 10.1080/00396265.2019.1583848.

18. Varbla, S.; Ellmann, A.; Delpeche-Ellmann, N. Validation of marine geoid models by utilizing hydrodynamic model and shipborne GNSS profiles. *Marine Geodesy* 2020, 43(2), 134–162, doi: 10.1080/01490419.2019.1701153.

19. Liibusk, A.; Ellmann, A.; Kõuts, T.; Jürgenson, H. Precise hydrodynamic levelling by using pressure gauges. *Marine Geodesy* 2013, 36(2), 138-163, doi: 10.1080/01490419.2013.771594.

20. Cipollini, P.; Francisco M.C.; Jevrejeva, S.; Melet, A.; Prandi, P. Monitoring Sea Level in the Coastal Zone with Satellite Altimetry and Tide Gauges. *Surveys in Geophysics* 2017, 38, 33–57, doi: doi.org/10.1007/s10712-016-9392-0.

21. Wingham, D.J.; Rapley, C.G.; Griffiths, H. New techniques in satellite altimeter tracking systems. In Proceedings of IGARSS 1986, 86, 1339-1344.

22. Chander, S.; Ganguly, D.; Dubey, A.K.; Gupta, P.K.; Singh, R.P.; Chauhan, P. Inland water bodies monitoring using satellite altimetry over Indian region. 2014, International Archives of the Photogrammetry, Remote Sensing & Spatial Information Sciences.

23. Kollo, K.; Ellmann, A. Geodetic Reconciliation of Tide Gauge Network in Estonia. *Geophysica* 2019, 54(1), 27−38.

24. Nordman, M.; Kuokkanen, J.; Bilker-Koivula, M.; Koivula, H.; Hakli, P.; Lahtinen, S. Geoid Validation on the Baltic Sea Using Ship-borne GNSS Data. *Marine Geodesy* 2018, 41(5), 457-476, doi: 10.1080/01490419.2018.1481160.

25. Varbla, S.; Ellmann, A.; Märdla, S.; Gruno, A. Assessment of marine geoid models by ship-borne GNSS profiles. *Geodesy and Cartography* 2017, 43(2), 41−49, doi: 10.13140/RG.2.2.32537.11365.

26. Estey, L. H.; Meertens, C. M. TEQC: the multi-purpose toolkit for GPS/GLONASS data. *GPS Solutions* 199, 3(1), 42-49, doi: 10.1007%2FPL00012778.

27. Kall, T.; Oja, T.; Kollo, K.; Liibusk, A. The Noise Properties and Velocities from a Time-Series of Estonian Permanent GNSS Stations. *Geosciences* 2019, 9(5), 1−23, doi: 10.3390/geosciences9050233.

28. Pujol, M-I., Mertz, F. Product User Manual, Tech. rep., Copernicus Marine Environment Monitoring Service. 2020, https://resources.marine.copernicus.eu/documents/PUM/CMEMS-SL-PUM-008-032-062.pdf.

29. Axell, L., Huess, V. Product User Manual, Tech. rep., Copernicus Marine Environment Monitoring Service. 2020, https://resources.marine.copernicus.eu/documents/PUM/CMEMS-BAL-PUM-003-011.pdf.

30. Liu, Y.; Axell, L.; Jandt, S.; Lorkowski, I.; Lindenthal, A.; Verjovkina, S.; Schwichtenberg, F. Quality Information Document, Tech. rep., Copernicus Marine Environment Monitoring Service. 2019, https://resources.marine.copernicus.eu/documents/QUID/CMEMS-BAL-QUID-003-011.pdf.

31. Madsen, K.S.; Høyer, J.L.; Suursaar, Ü.; She, J.; Knudsen, P. Sea level trends and variability of the Baltic Sea from 2D statistical reconstruction and altimetry. *Frontiers in Earth Science* 2019, 7(243), 1−12, doi: 10.3389/feart.2019.00243.

32. Li, P.; Li, H.; Chen, F.; Cai, X. Monitoring Long-Term Lake Level Variations in Middle and Lower Yangtze Basin over 2002–2017 through Integration of Multiple Satellite Altimetry Datasets. *Remote Sensing* 2020, 12(9), 1448, doi: 10.3390/rs12091448.

33. Cretaux, J.F.; Berge-Nguyen, M.; Calmant, S.; Jamangulova, N.; Satylkanov, R.; Lyard, F.; et al. Absolute calibration or validation of the altimeters on the Sentinel-3A and the Jason-3 over Lake Issykkul (Kyrgyzstan). *Remote Sensing* 2018, 10(11), 1679, doi: 10.3390/rs10111679.

34. Suursaar, Ü.; Kall, T. Decomposition of Relative Sea Level Variations at Tide Gauges Using Results From Four Estonian Precise Levelings and Uplift Models. *IEEE Journal of Selected Topics in Applied Earth Observations and Remote Sensing* 2018, 11(6), 1966−1974, doi: 10.1109/JSTARS.2018.2805833.

35. Xu, Q.; Cheng, Y.; Plag, H-P.; Zhang, B. Investigation of sea level variability in the Baltic Sea from tide gauge, satellite altimeter data, and model reanalysis. *International Journal of Remote Sensing* 2014, 36(10), 2548-2568, doi: 10.1080/01431161.2015.1043405.

36. Madsen, K.S.; Høyer, J.L.; Tscherning, C.C. Near-coastal satellite altimetry: Sea surface height variability in the North Sea–Baltic Sea area. *Geophysical Research Letters* 2007, 134, L14601, doi:10.1029/2007GL029965